

Facile fabrication of multifunctional superoleophobic and antifouling metal mesh by dip-coating polyanion for efficient oil/water mixtures as well as emulsions separation

Chao Yang^a, Jun Yang^a, Ge Song^a, Limin Zang^{a,*}, Qifan Liu^b, Jianhui Qiu^b, Xue Yang^{c,*}, Chun Wang^a

^aKey Laboratory of New Processing Technology for Nonferrous Metal and Materials (Ministry of Education) and College of Materials Science and Engineering, Guilin University of Technology, Guilin 541004, China, Tel. +86 773 5896672; emails: 2016034@glut.edu.cn (L. Zang), yangchao_chem@163.com (C. Yang), yjun013@gmail.com (J. Yang), songe16@126.com (G. Song), 2974321276@qq.com (C. Wang)

^bDepartment of Machine Intelligence and Systems Engineering, Faculty of Systems Science and Technology, Akita Prefectural University, Yurihonjo 015-0055, Japan, Tel. +81 184 272134; emails: liuqifan0108@gmail.com (Q. Liu), qiu@akita-pu.ac.jp (J. Qiu)

^cDepartment of Anesthesiology, Huashan Hospital, Fudan University, Shanghai 200040, China, Tel. +86 2152887649; email: yangxue5611@126.com (X. Yang)

Received 26 August 2019; Accepted 24 January 2020

ABSTRACT

Oil/water separation has recently attracted a great deal of attention for research due to the frequent occurrence of an oil spill as well as the increase of industrial and household oily wastewater. Therefore, the purpose of this study is to demonstrate underwater superoleophobic cross-linked phosphorylated poly(vinyl alcohol) hydrogel coated stainless steel mesh (CL-PPVA@SSM), which was fabricated using a simple dip-coating method and aldol reaction on the mesh substrate. The as-prepared CL-PPVA@SSM is capable of separating oil from a variety of different oil/water mixtures with high separation efficiency up to 99.2%, excellent recyclability and fast water permeate flux of 467.7 L m⁻² h⁻¹, which makes it suitable for the separation of oil-water mixtures from oil-water emulsions. Also, in the oil-water separation process, the CL-PPVA@SSM is capable to remove organic dye from the water. The CL-PPVA@SSM exhibits stability under various harsh conditions such as mechanical abrasion. Importantly, the CL-PPVA@SSM shows a massive potential to separate kitchen waste oil/water mixtures due to the underwater superoleophobic property as required for the recycling of kitchen waste oil. Therefore, this method has been met with a promising application prospect of practical application.

Keywords: Phosphorylated poly (vinyl alcohol); Special wettable materials; Kitchen waste oil; Superhydrophilic surface; Oil-water separation

1. Introduction

With the rapid development of society and industrialization, water pollution caused by the leak of oils, dyes and domestic sewage has become an increasingly serious problem encountered by human beings [1,2]. The recovery and

treatment of industrial and civil oily wastewater is a universal challenge. The environmental, economic and social demands emphasize the need for materials that can separate water and oil simply and effectively for treatment and subsequent use [3]. The efficient separation of oil/water mixtures discharged remains faced with various technical difficulties [4].

* Corresponding authors.

Recently, the technology of oil-water separation is a new approach based on special wettable materials that have been demonstrated to be very appropriate for an oil spill. Moreover, plenty of novel technologies have been developed to realize oil/water separation, such as plasma treatment [5], electrospinning [6], spraying-coating [7], vapor-liquid interfacial reaction [8], electrodeposition [9], and femtosecond laser technology [10]. Nevertheless, all of the aforementioned technologies have been reported to show such drawbacks as high energy consumption, complex process and hefty machining cost, all of which are adverse to the practical application of them in oil/water separation. At present, there are two major types of special wettable materials that have been applied to oil/water separation. They are superoleophilic or superhydrophobic materials (oil removing) and underwater superoleophobic superhydrophilic materials (water removing) [3,11–13].

As for the “oil removing” materials, it is easy for oil to pass through, with the water retained on the surface. However, these oleophilic surfaces are susceptible to blockage or pollution due to the presence of oil. In comparison, “water removing” materials allow the oil to be retained on the surface, which thus makes it easy for the water to pass through [11]. During the separation process enabled by “water removing” materials, the underwater superoleophobic interface with low adhesion for oil drops prevents the coated substrate from fouling by oil, which facilitates the recycling of oil and materials [14]. Through comparison with traditional hydrophobic and oleophilic materials, it can be found out that the “water removing” materials with hydrophilicity could overcome the hard-recycling and easy-fouling limitations.

Hydrogel is known as a variety kind of typical hydrophilic materials, which consists of an interconnected network with water filling the interstitial spaces. Due to its excellent ability to hold and absorbing water, a hydrogel is considered as suitable for the design of novel oil/water separation materials [15–19]. In this study, the mesh that performs the function of separation is fabricated with hydrophilic hydrogel coatings for the highly efficient separation of oil/water mixtures. The interconnected phosphorylated poly(vinyl alcohol) (CL-PPVA), was chosen as the cladding material, where glutaraldehyde was taken as the chemical cross-linker. Stainless steel mesh (1,000 mesh) was taken as the substrates. Unlike the crosslinked poly(vinyl alcohol) hydrogel, CL-PPVA hydrogel contains a large number of hydroxyls and phosphate groups. These groups enable the separation of wastewater that contains emulsified oils.

This study proposes an underwater superhydrophobic, superhydrophilic, and anti-oil adhesion PPVA@SSM using an effective and simple dip-coating method. The PPVA@SSM exhibits high selectivity for the separation of water from oil-water mixtures. Additionally, the CL-PPVA@SSM exhibits stability under various harsh conditions, for instance, mechanical abrasion. Importantly, the CL-PPVA@SSM demonstrates the capability to adsorb organic dyes synchronously from water during the process of oil-water separation. Besides, it shows an enormous potential to separate kitchen waste oil/water mixtures due to the underwater superoleophobic property for the recycling of kitchen waste

oil. The present work suggests encouraging applications to various oil-water separation systems, benefiting the environmentally sustainable development and recycling of waste resources.

2. Materials and methods

2.1. Materials

Polyvinyl alcohol (polymerization degree is 1,700 and alcoholysis degree is 99%), dicyandiamide, phosphoric acid, N,N-dimethylformamide (DMF), urea, glutaraldehyde, methylene blue, sodium dodecyl sulfate (SDS), sodium hydroxide, vitriol, sodium chloride, kerosene, xylene, liquid paraffin, cyclohexane, dichloromethane, and vacuum pump oil were purchased from the Aladdin Bio-Chem Reagent Co., Ltd., China. Kitchen waste oil was sourced from the local college canteen. All of the reagents were of analytical grade and were used without any further purification. Rapeseed oil, stainless steel mesh (2,300 mesh) and sandpaper (Grit No. 400) were obtained from the local market. The stainless steel mesh was cut into 50 × 50 mm pieces and then washed by distilled water, acetone and alcohol respectively before use.

2.2. Samples preparation

The first step was to prepare of the highly phosphorylated poly(vinyl alcohol) (PPVA). PPVA was obtained from the phosphorylation of PVA with phosphoric acid according to the reference method of the related reference as follows [20–22]: to a solution of urea (15 g) and dicyandiamide (10 g) in 50 ml of DMF, phosphoric acid (10 ml) was added. The solution was heated at 130°C, before the addition of PVA (6 g). The reaction solution was stirred for 80 min at 130°C. The aforementioned solution was dialyzed against deionized water through Visking cellulose tubing for 24 h to remove any surplus reagents. A powder of PPVA was obtained by incrementally adding alcohol to the dialyzed PPVA aqueous solution with vigorous agitation. The precipitate was filtered, washed with alcohol, and then dried at 30°C.

The second step was to prepare cross-linked PPVA hydrogel@stainless steel mesh. The hydrogel-coated SS mesh was prepared using an easy dip-coating method and crossing reaction. In a typical process, the pretreated SS mesh was dipped into the PPVA aqueous solution (0.5 wt.%) at normal temperature for 2 min, thus allowing the PPVA solution to wet the SS mesh thoroughly. Then, it was taken out horizontally to remove the excess impregnation solution left from SS mesh. Subsequently, a glutaraldehyde solution (25 wt.%) was sprayed on both sides of the PPVA-coated SS mesh using a spray bottle. Following the cross-linked process, the mesh was washed by distilled water and then dried in an oven at 50°C to obtain the crosslinked PPVA coated SS mesh named CL-PPVA@SSM.

2.3. Oil-water separation performance of CL-PPVA@SSM

A variety of oils, including chloroform, kerosene, xylene, liquid paraffin, and cyclohexane, dichloromethane,

and pump oil were involved in this study. A piece of the CL-PPVA@SSM was fixed under a glass funnel in horizontal, before prewetting with water. The oil-water mixture [selected oil (dyed with Red G, 40 mL) and water (40 mL)] was poured into the above-mentioned funnel.

During the separation process, gravity is the only driving force. The surfactant-stabilized oil-in-water emulsion was prepared by mixing 50 mg SDS, 1 mL oil (liquid paraffin, kerosene, xylene, cyclohexane, and pump oil), and 99 mL water under 3 h of magnetic stirring and ultrasonic dispersion for 1 h. The separation efficiency was calculated by the oil rejection coefficient (R) according to [23]:

$$R = \left(1 - \frac{C_a}{C_b}\right) \times 100\% \quad (1)$$

where C_a and C_b indicate the weight of water before and after one-off separation, respectively. The flux J was estimated by measuring the time for a constant flow according to Eq. (2) [23]:

$$J = v \times (a \times \Delta t)^{-1} \quad (2)$$

where a represents the effective membrane area, Δt indicates the filtration time and v denotes the volume of filtering water.

2.4. Dye removal and mechanical stability of CL-PPVA@SSM

A piece of CL-PPVA@SSM (50 mm × 50 mm) was immobilized on the glass slide with flange the oil-water mixture was obtained through the addition of cyclohexane (40 mL, dyed with Red G) into 40 mL of water (dyed with MB). Subsequently, the concentrations of MB were measured before and after the process of separation, respectively.

The surface of CL-PPVA@SSM was placed face-down to the sandpaper. This surface was transversely and longitudinally abraded 10 cm for each direction by the sandpaper under a metal block at 100 g such process was treated as

one cycle. Such a process was named as one cycle. After the cycle's abrasion test, the underwater oil contact angles and separation efficiency were measured.

2.5. Characterization

The Fourier transform infrared (FT-IR) spectroscopy measurements (Impact 400, Nicolet, Waltham, MA) were performed using the KBr pellet method. The surface morphologies of the samples were investigated by field emission scanning electron microscope (SEM; S4800, HITACHI, Japan) at an accelerating voltage of 5.0 kV. The surface wettability of the sample evaluated using a contact angle goniometer (JY-PHb, Chende Jinhe, China) at room temperature. The contact angle, underwater oil contact angle and the sliding angle measured in line with the relevant reference standards [23], as shown in Fig. S1 in the Supporting Information. The concentrations of methylene blue were obtained by spectrophotometry with the assistance of a UV-Vis spectrometer (9000S, Metash Instrument Co., Ltd, China).

3. Results

3.1. Fabrication and characterization of the CL-PPVA@SSM

The PPVA hydrogel-coated SS mesh was fabricated by following a simple dip-coating and crosslinking process. The preparation process is illustrated in Fig. 1. Clean SS mesh was dipped into a PPVA solution (0.5 wt.%) for roughly 1 min, before being taken out horizontally from the PPVA solution. Subsequently, glutaraldehyde aqueous solution (25 wt.%) was sprayed onto both sides of the PPVA coated SS mesh with a spray bottle to obtain the crosslinked PPVA hydrogel-coated SS mesh (CL-PPVA@SSM).

The hydrogel was capable of sticking to the SS mesh tightly without the need for any other adhesives, which is attributed to the high viscosity of the PPVA solution before the crosslinking process. The viscosity of PPVA solution (0.5 wt.%) reached 424.0 mPa s at 25°C. Relatively, the viscosity of PVA solution (0.5 wt.%) was lower than 1.0 mPa s.

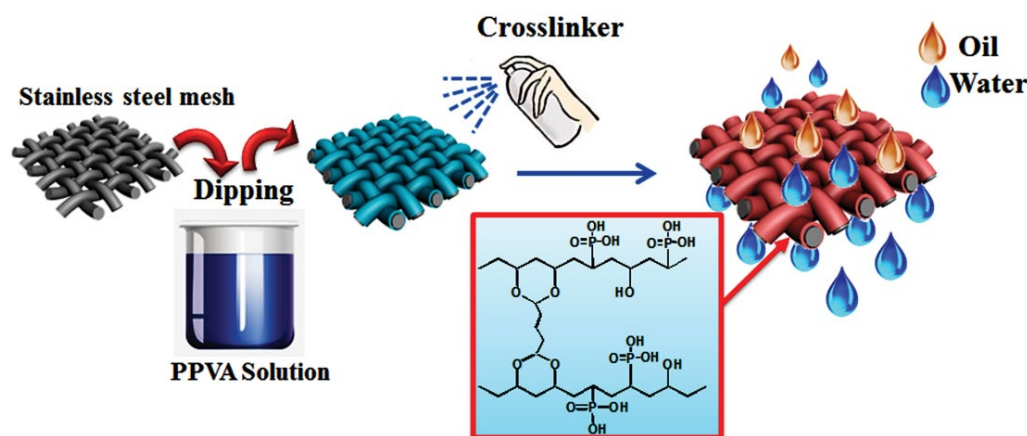


Fig. 1. Schematic illustration of the preparation process of crosslinked PPVA hydrogel-coated SS mesh.

Over the course of acetalization, the hydroxyl groups on PPVA underwent reaction with the aldehyde groups of glutaraldehyde, thus increasing the crosslink bonds between the PPVA chains. For the determination of acetalization, the FT-IR spectra of PPVA and crosslinked PPVA hydrogel were compared as shown in Fig. 2. The new absorption peaks at 938 and 1,225 cm^{-1} were observed. These absorption peaks at 938 and 1,225 cm^{-1} were the characteristic absorption of the P–O–C symmetric stretching vibration and P=O stretching vibration in PPVA. For the CL-PPVA, the absorption peak at 1,012 cm^{-1} was the characteristic absorption of the C–O–C group in cross-linked PPVA.

The surface morphologies of the meshes either before or after the treatment by CL-PPVA were observed by SEM. In Fig. 3a, there are plenty of crazing's observed on the surface of the raw SS mesh, which would facilitate the passage of liquids. A smooth surface on the SS mesh is found available under high magnification (Fig. 3b). The morphologies of CL-PPVA@SSM were shown in Fig. 3c and d. Obviously, the SS mesh was covered with a thin layer of CL-PPVA hydrogel. Furthermore, the cracks were exempt from blockage by the hydrogel. To confirm that the thin layer of a hydrogel of CL-PPVA@SSM cannot dissolve easily in water, the CL-PPVA@SSM was repeatedly immersed in hot water and washed 10 times by the deionized water characterized by EDS. The element mappings of P, C, O, and Fe are shown in Fig. 3e, respectively. As the main components of CL-PPVA hydrogel, carbon, oxygen, and phosphorus were distributed uniformly on the SS mesh.

3.2. Anti-oil adhesion and underwater superoleophobicity of CL-PPVA@SSM

It is widely known that the chemical composition of the material is one of the major influencing factors for the wettability of a solid surface. A hydrophilic CL-PPVA hydrogel that contains a substantial amount of hydroxyls and phosphate groups, coating of the SS mesh affords a feasibility for the manufacture of underwater superoleophobic mesh. The wettability of oil and water on CL-PPVA coated mesh was

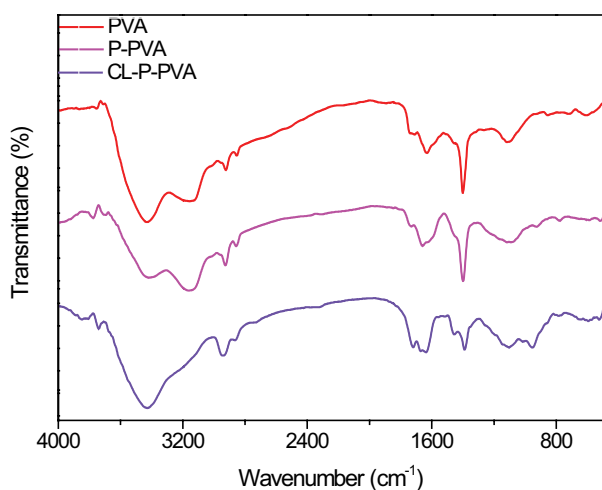


Fig. 2. FTIR spectra of PVA, PPVA, and cross-linked PPVA.

estimated by the contact angle. For comparison purposes, the wettability of crosslinked PVA hydrogel coated SS mesh was characterized as well.

As shown in Fig. 4a, water droplet permeates the entire CL-PPVA@SSM surface, thus forming a water contact angle (WCA) of 0° in air, which indicates its superior superhydrophilicity. After permeation in water, the underwater oil contact angle (UWOCA) of a dichloromethane droplet on the surface of the CL-PPVA@SSM reached 154.1° (Fig. 4b), which suggested its underwater superoleophobicity (UWOCA > 150°). To compare the degree of superhydrophilicity, the WCA in the air of the raw SS mesh was set to 112.9° (Fig. 4c), the underwater dichloromethane CA of the raw SS mesh was set to 111.4° (Fig. 4d), the WCA in the air of the CL-PVA@SSM was set to 63.0° (Fig. 4e) and the underwater dichloromethane CA of the CL-PVA@SSM was set to 127.5° (Fig. 4f), which implied that the phosphate groups on side-chain of PVA played a significant role in enhancing the underwater superoleophobicity of a hydrogel. Also, the UOCAs of various oils were measured, which led to the finding that all the UOCAs exceeded 150°, as shown in Fig. 5.

To gain a better understanding of the wettability and underwater superoleophobicity of the CL-PPVA@SSM, the general mechanism of action of wettability on UOCAs can be explained by the Eq. (3) [23]:

$$\cos \theta_{ow} = \frac{\gamma_{oa} \times \cos \theta_{oa} - \gamma_{wa} \times \cos \theta_{wa}}{\gamma_{ow}} \quad (3)$$

where θ_{ow} and γ_{ow} represent the contact angle and surface tension of oil in water, water in air and oil in water. θ_{oa} and γ_{oa} represent the contact angle and surface tension of oil in water. θ_{wa} and γ_{wa} denote the contact angle and surface tension of water in the air. When the oil is identical, γ_{oa} , γ_{wa} and θ_{oa} are constant in general. The θ_{ow} shows a declining trend with the increase of θ_{wa} , which means that, the substrate is more hydrophilic, and that it is more oleophobic underwater. For CL-PPVA@SSM, there are numerous phosphate groups and hydroxyls of the CL-PPVA. The hydration layer will form on the surface of CL-PPVA@SSM, which can lead to such a high level of superhydrophilicity and underwater superoleophobicity.

The adhesion properties have been studied for the further application of oil/water separation meshes. In practice, oil adhesion would cause contamination of the mesh, which further causes the loss of selectivity. In general, the strong hydration layer exhibits more excellent oleophobicity and greater resistance to anti-oil adhesion. To investigate the resistance of CL-PPVA@SSM to oil adhesion, the sliding angle (SA) was measured. The angle at which the liquid drop began to slide on the gradually inclined surface is defined as the sliding angle.

As shown in Fig. 6, the underwater SA (dichloromethane) on the surface of CL-PPVA@SSM was < 5° and the dichloromethane droplet rolled off lightly. In comparison, the underwater SA (dichloromethane) of the raw SS mesh was 90° and the dichloromethane droplet remained attached to raw SS mesh. It did not roll off (Fig. 6b) even when the raw SS mesh was in a vertical position. In water, the hydrogel coatings on the surface of CL-PPVA@SSM absorbed water to reach its balanced state. When the oil droplets made contact

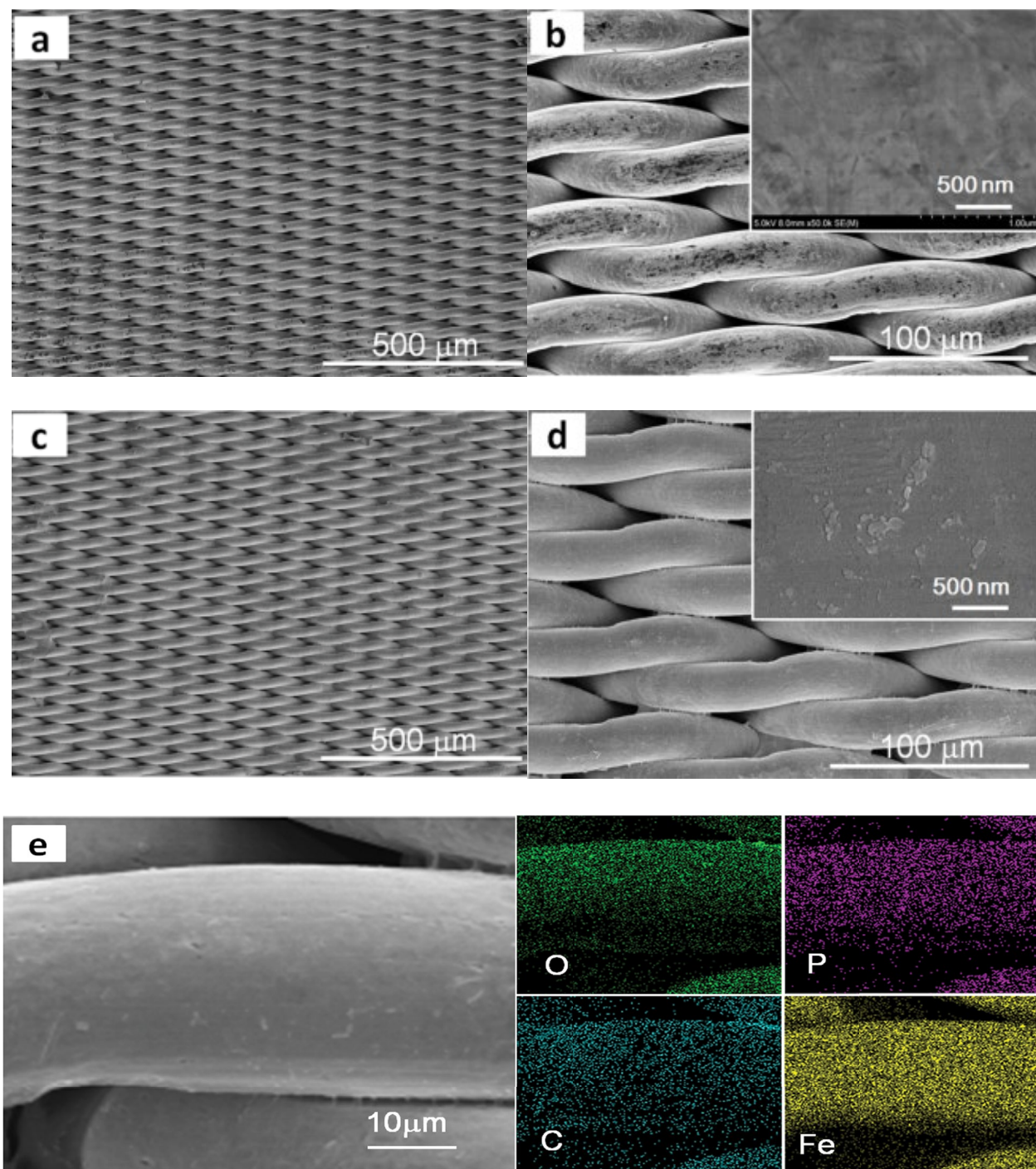


Fig. 3. SEM images of SSM (a) low magnification, (b) enlarged view; SEM images of CL-PPVA@SSM (c) low magnification, (d) enlarged view, and (e) element mappings of P, C, Fe, and O, respectively.

with the hydrogel, an oil/water/solid ternary composite interface was immediately formed. These trapped water molecules on this interface would cause a significant reduction in the contact area between the solid surface and oil droplet. As a result, it is easy for the oil droplet to roll off the CL-PPVA@SSM.

The established oil-contacting method can be applied to investigate the low adhesion of the CL-PPVA@SSM [24].

The adhesion behavior exhibited by the CL-PPVA@SSM was tested by separating a 5 μ L oil droplet from its surface. Fig. 7 shows the dynamic process, including approach, contact, pressure, and departure. Apparently, the oil droplet can lightly and decisively away from the surface even when the droplet was compressed onto the surface of CL-PPVA@SSM, indicating its remarkable anti-adhesion property.

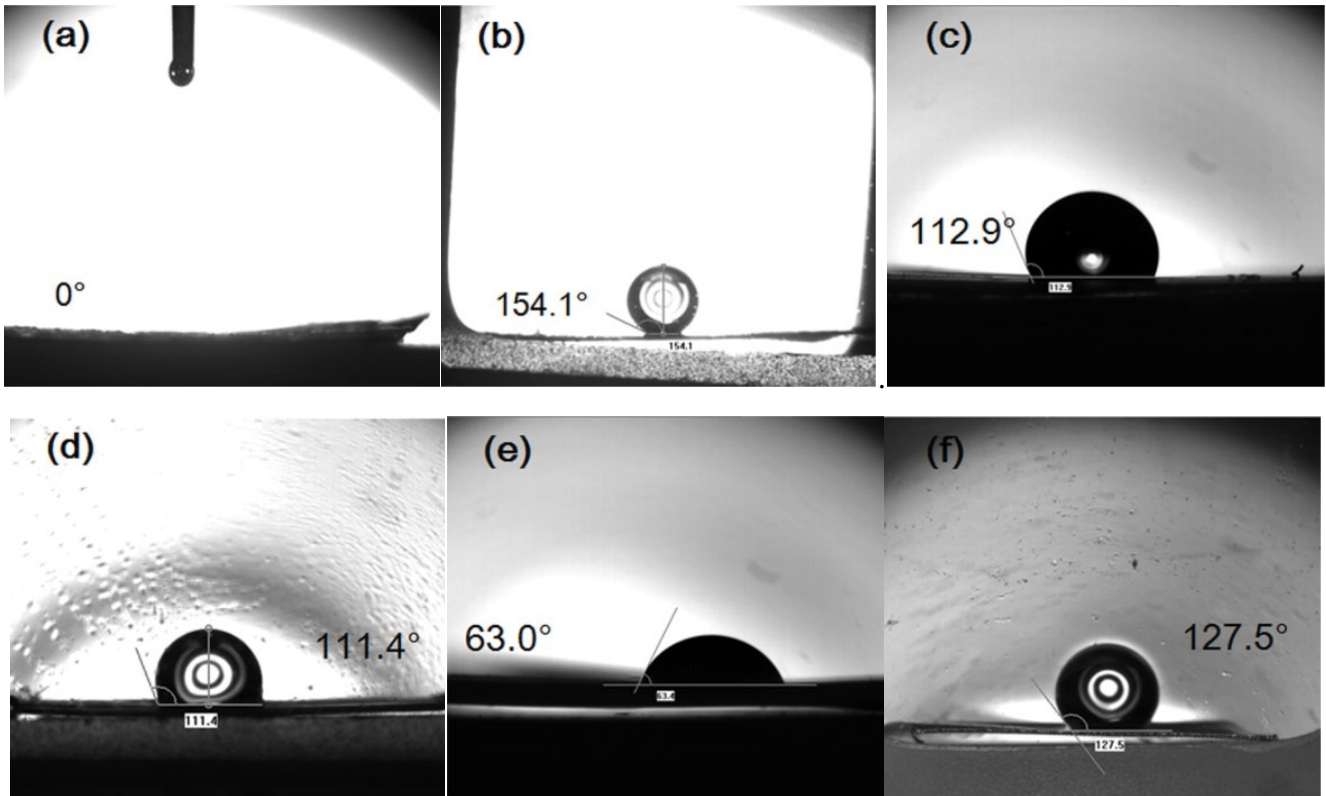


Fig. 4. Water contact angle (WCA) and the UWOCA of the (a and b) CL-PPVA@SSM, (c and d) CL-PVA@SSM (e and f) and raw SS mesh, respectively.

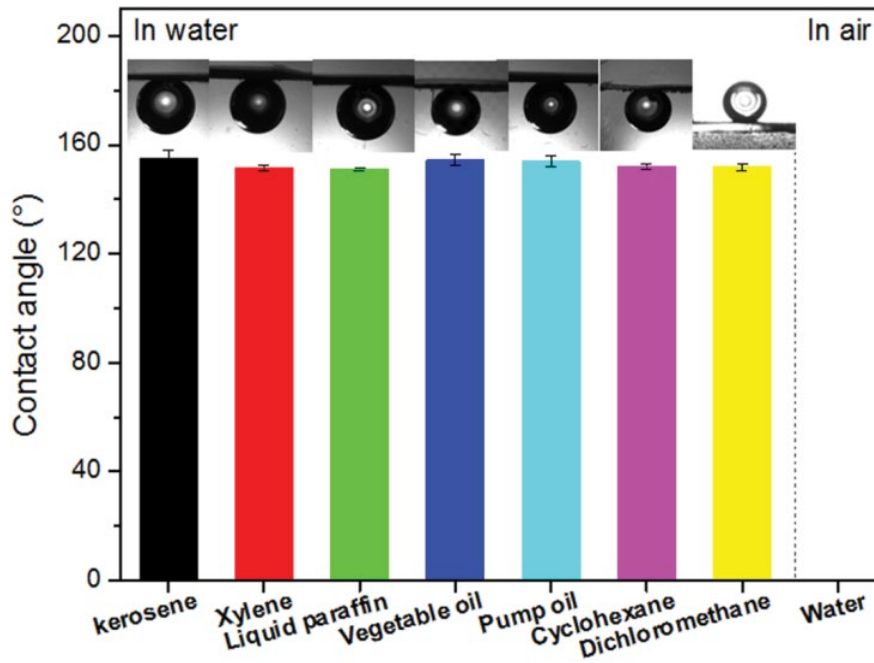


Fig. 5. Underwater oil contact angles of various oils.

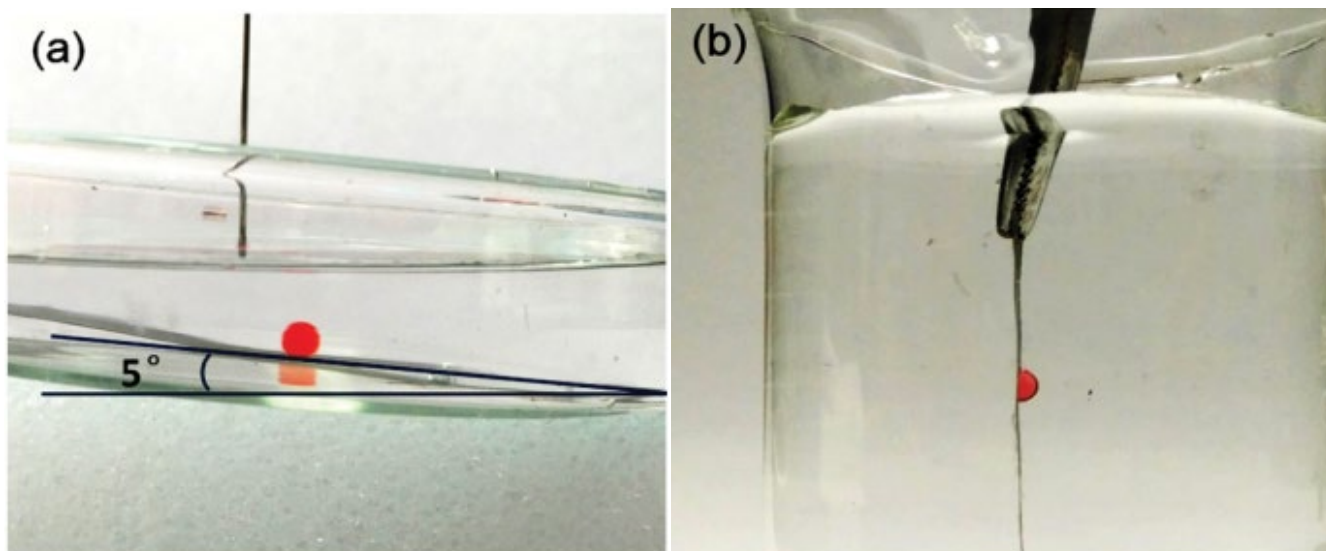


Fig. 6. Underwater dichloromethane sliding angles of the (a) CL-PPVA@SSM and (b) raw SS mesh.

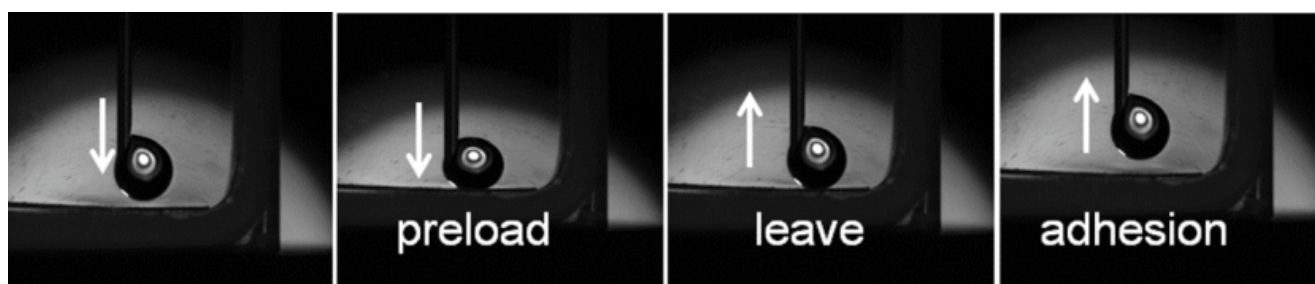


Fig. 7. Adhesion behavior of the CL-PPVA@SSM (the direction of the arrow indicates the movement of the oil droplet).

The low underwater oil adhesion is evidenced by the anti-oil-fouling and water-rinsing performance. The CL-PPVA@SSM was immersed in liquid paraffin and vegetable oil and then was rinsed in water as shown in Fig. 8. As revealed by the experimental results, cleanliness was restored to the fouled CL-PPVA@SSM. By contrast, the raw SS mesh could not be made clean after being polluted by the same oils, which indicates that the CL-PPVA@SSM possesses excellent self-cleaning property and greater resistance to oil adhesion in water. During the process of oil-water separation, the CL-PPVA@SSM is easier to clean after being stained.

3.3. Separation capability tests

To further evaluate the capability of oil-water separation, the CL-PPVA@SSM was used in the experiment of a selective oil-water separation. Before being fixed horizontally under a glass funnel, the CL-PPVA@SSM was pre-wetted with little water (~200 μL) as shown in Fig. 9a. Subsequently, a mixture of water (30 mL) and kerosene (30 mL, dyed with Red G) was poured into the glass funnel. During the process of oil-water separation, only the water permeated the CL-PPVA@SSM. In comparison, both the kerosene and the water permeated SSM-coated PPVA without cross-linking,

which can be attributable to the high solubility of PPVA without cross-linking.

The CL-PPVA@SSM demonstrated excellent superhydrophilicity and underwater superoleophobicity, which could enable it to absorb the water floating on oil. A miniature boat was made in the CL-PPVA@SSM to evaluate the capability of water removal ability from the oil surface. As shown in Fig. 9b, the boat could float on the surface of dichloromethane containing water in a container due to its underwater superoleophobicity. The water could quickly wet and permeate the mesh owing to its superhydrophilicity. The miniature boat could avoid sinking into dichloromethane even when it was filled with water. Obviously, this separation process was a simple one, as the water collected into the boat could be sucked with a dropper.

As for the CL-PPVA@SSM, it allows water to flow through rapidly. Meanwhile, the oils are retained above the CL-PPVA@SSM. Due to gravity, the entire process of separation can occur spontaneously. The water flux can be used to evaluate the separation efficiency of the separation mesh. As shown in Fig. 10a, the rate at which the water was separated from the oil-water mixture reached 99.2% for the first trial and the water permeate flux reached $467.7 \pm 0.5 \text{ L m}^{-2} \text{ h}^{-1}$ [25–28]. Moreover, the CL-PPVA@SSM could be recycled due to its self-cleaning ability. As shown in Fig. 10b, the

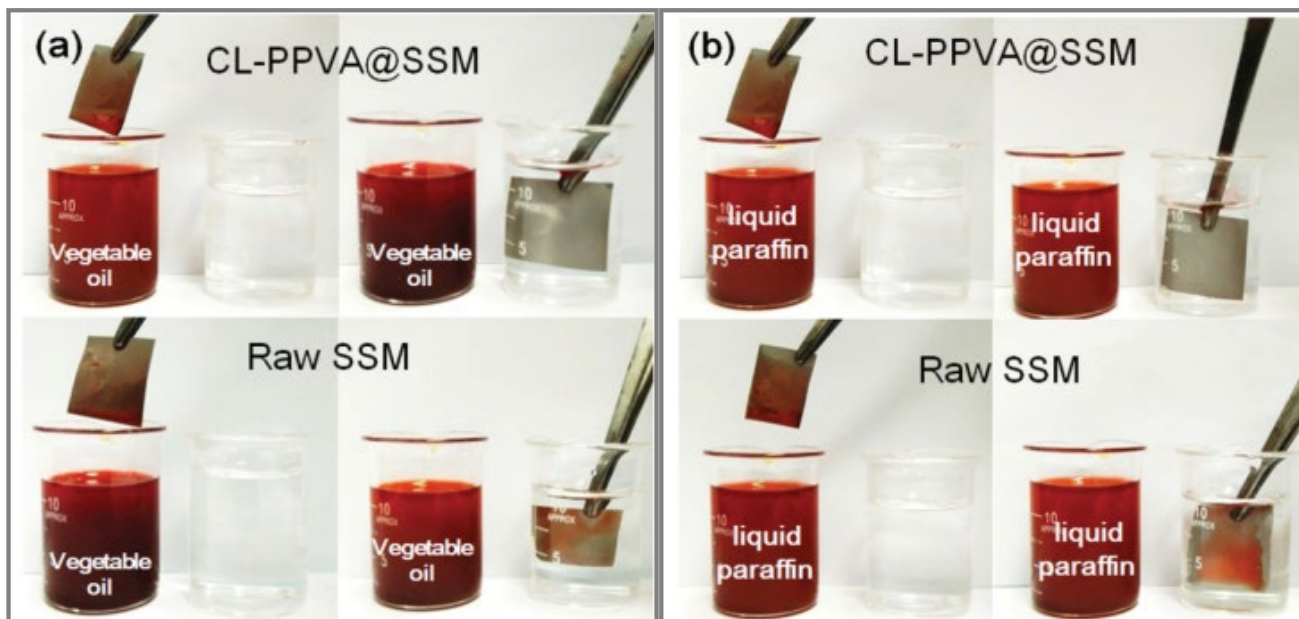


Fig. 8. Anti-oil-fouling and water-rinsing performance of (a) CL-PPVA@SSM and (b) raw SS mesh.

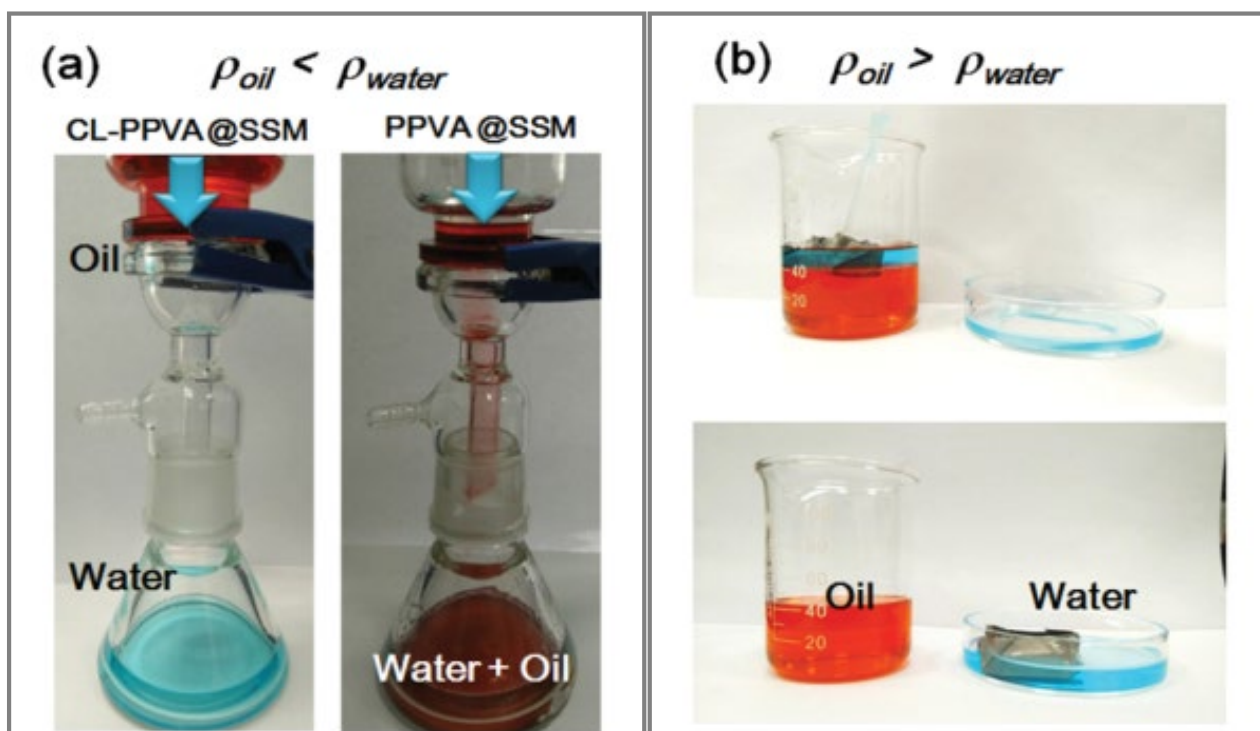


Fig. 9. (a) Oil-water separation capability of CL-PPVA@SSM and PPVA@SSM; (b) the collection process of water (dyed blue) from dichloromethane (dyed red) by a miniature box made of the CL-PPVA@SSM.

separation performance of CL-PPVA@SSM, including the water permeate flux and the separation efficiency remained broadly unchanged after 10 cycles. The above-mentioned results demonstrate that the CL-PPVA@SSM was quite effective and suitable for the practical application in the field of wastewater treatment. Besides, oil (kerosene) intrusion

pressure was involved to evaluate the separation capacity of CL-PPVA@SSM. The intrusion pressure (P) value was calculated using Eq. (4):

$$P = \rho \times g \times h_{\max} \quad (4)$$

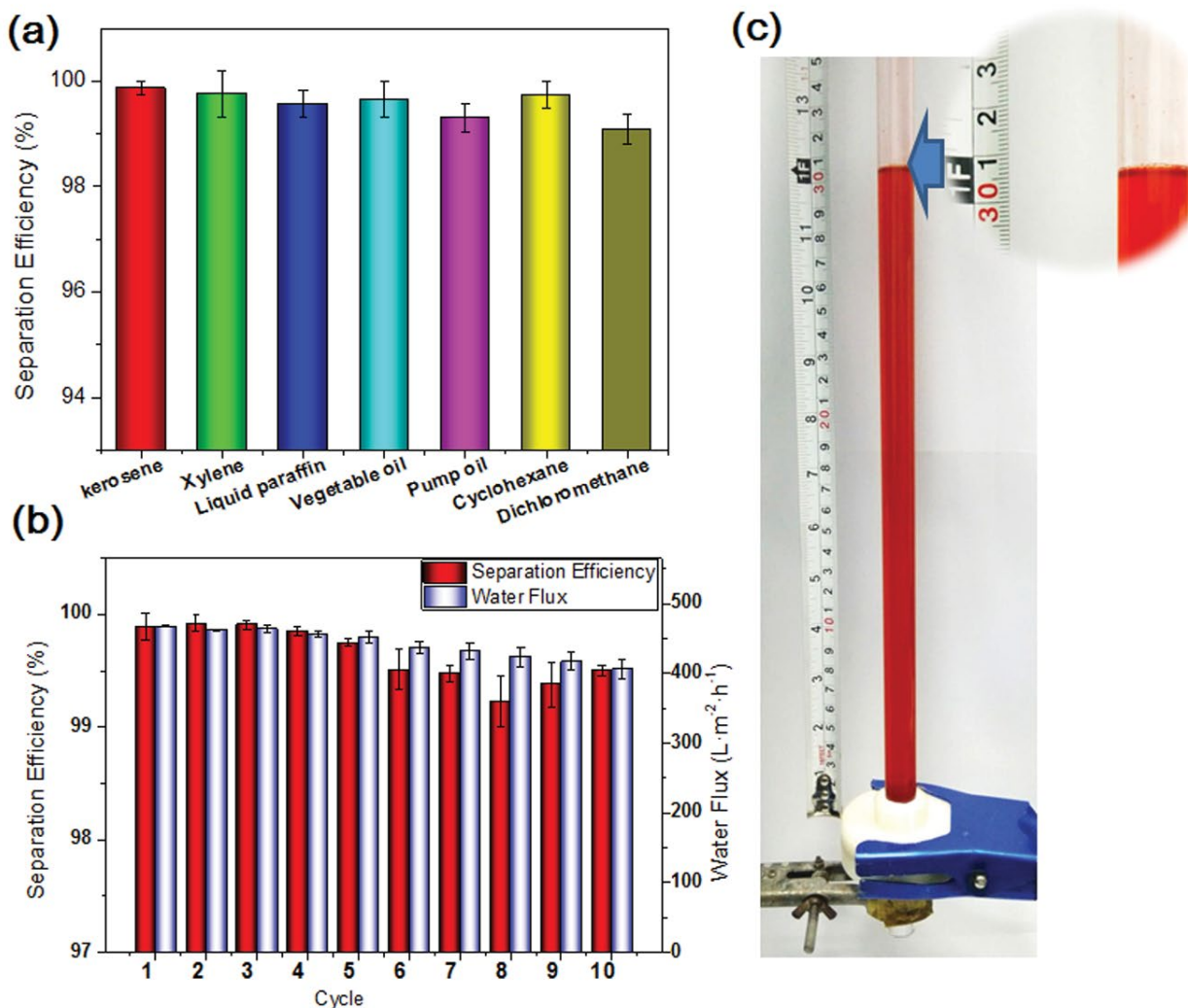


Fig. 10. (a) Separation efficiency of the oil/water mixtures; (b) the water flux of the CL-PPVA@SSM for separating kerosene /water mixtures in the ten cycles and (c) the intrusion pressure of oil taking kerosene as an example.

where g represents gravitational acceleration, ρ indicates the density of the oil, and h_{\max} denotes the maximum height of oil the CL-PPVA@SSM can support. The average h_{\max} is 30.5 cm, and kerosene is incapable to flow through the mesh under the pressure ($P = 2.4$ kPa), as shown in Fig. 10c.

In order to evaluate the capability of water-oil separation of the CL-PPVA@SSM, the emulsion separation test was conducted [29]. The CL-PPVA@SSM was pre-wetted up by water and sandwiched between flanges, as illustrated in Fig. 11. The oil-in-water emulsion poured from the upper tube was transformed into clear water droplets after separation, which was received in a vessel below. Due to the presence of gravity, the entire process of separation can occur spontaneously. The microscopic images of emulsions before and after separation are presented in Figs. 11b and c, respectively. Compared to the emulsion, there was no oil droplet discovered in the separated water, which led to a clear solution. A series of results of oil/water emulsion separation tests have clearly demonstrated that the CL-PPVA@SSM has high separation efficiency as shown

in Fig. S2. For comparison purposes, the water-oil separation capability of crosslinked PVA hydrogel coated SS mesh was investigated as well under the identical conditions and the results are presented in Fig. S3. It can be seen clearly in Fig. S3 that there is a noticeable difference in the outcome of separation between CL-PPVA@SSM and CL-PVA@SSM. The water-oil separation capability of CL-PVA@SSM is less than satisfactory, which could be attributable to the hydrophilic CL-PPVA hydrogel that contains a large number of phosphate groups.

3.4. Stability of CL-PPVA@SSM in harsh environments

The commonly-used oil-water separation materials are derived from organic polymer materials or inorganic-based materials. Therefore, they are supposed to withstand harsh environments. However, inorganic materials are prone to destruction in alkaline or acid medium while the organic polymer is unable to resist various organic solvents in general, which makes it necessary to maintain stable underwater

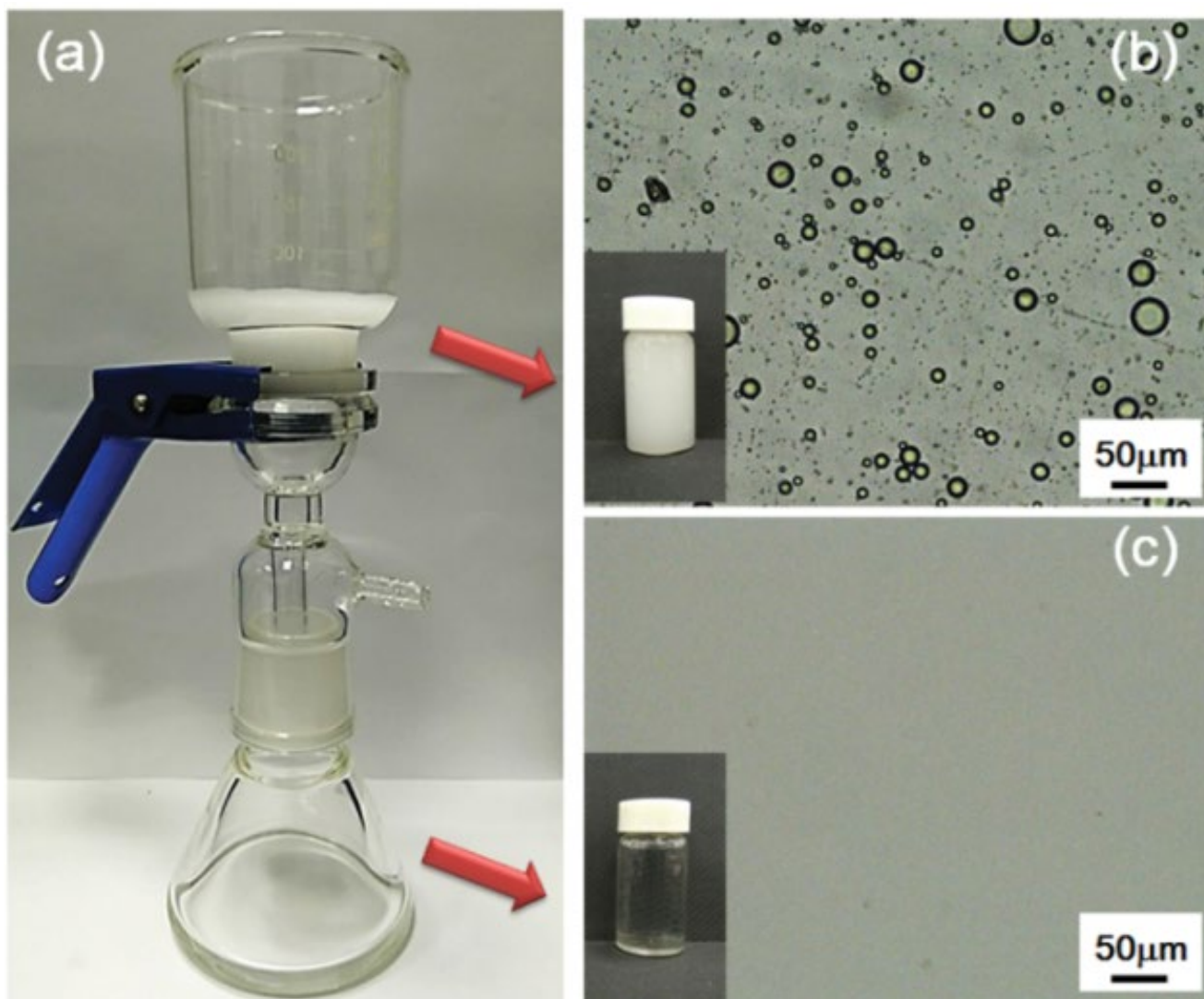


Fig. 11. (a) Separation experiment of hexane-in-water emulsion by the CL-PPVA@SSM; (b) optical microscopy images of surfactant-stabilized hexane-in-water emulsion and (c) water-in-hexane emulsion after separation.

superoleophobicity in some severe conditions [30]. The stability of the CL-PPVA@SSM was tested under extreme conditions such as acid/alkaline medium, organic solvents, and strong brine. In this study, the CL-PPVA@SSM was immersed in various corrosive organic solvents, 1 M NaOH, 1 M H_2SO_4 and saturated NaCl for 48 h, respectively. Subsequently, the UOCAs of soaked CL-PPVA@SSM were all more than 150° (Fig. 12a), which indicates that the oil-water separation mesh has excellent stability and is capable to withstand harsh conditions. It's worth noting that the CL-PPVA@SSM still maintains constant water flux and a high efficiency in oil-water separations after treatment in these harsh conditions.

For further evaluation of the robustness of the superhydrophilicity CL-PPVA@SSM surface against mechanical forces, an abrasion test was conducted as follows [23]. The test was carried out using 400-grit silicon carbide paper with the CL-PPVA@SSM facing the abrasion material. Meanwhile, the CL-PPVA@SSM was subject to a 100 g load and was

pulled in horizontal and vertical directions with a speed of 3 cm s^{-1} and an abrasion length of 20 cm. In particular, conspicuous surface scratches were not observed after 15 cycles, and the separation efficiency of CL-PPVA@SSM remained higher than 99.2% (Fig. 12b).

3.5. Multifunctional applications for CL-PPVA@SSM

In general, the discharge of wastewater containing waste dyestuffs and greasy dirt into rivers and lakes could be detrimental to the environment. In this study, it is assumed that the CL-PPVA@SSM could separate oils while absorbing dyes from wastewater over the course of oil-water separation. To validate this hypothesis, the MB concentration of aqueous phase before and after filtration was tested five times by UV-Vis Spectroscopy, as illustrated in Fig. 13. The intensity of the UV absorption peak of MB at 665 nm was significantly reduced after the filtration process, which

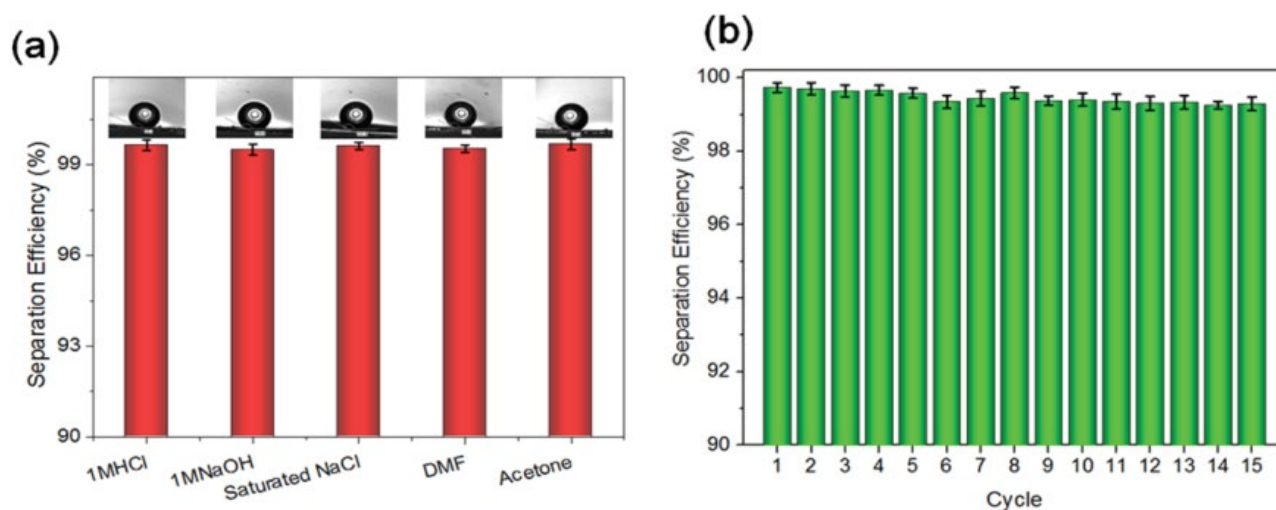


Fig. 12. (a) Separation experiments of CL-PPVA@SSM for mixtures of kerosene and various aqueous solutions; (b) cycling performance of CL-PPVA@SSM with abrasion test.

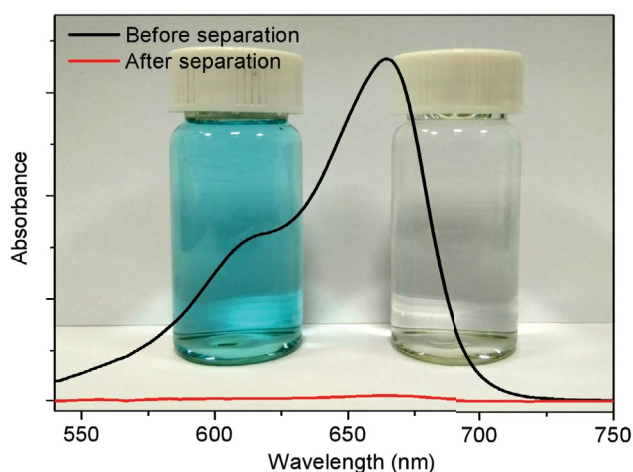


Fig. 13. UV-vis spectra of the MB aqueous solution before and after (5 cycles) filtration process.

suggests that the CL-PPVA@SSM is capable of dye removal. The amount of MB adsorption was attributed to the hydroxyl and anionic groups introduced into the surface of SS by crosslinked PPVA hydrogel. After five cycles of reuse, the separation effect of the CL-PPVA@SSM remained excellent, which implied that the CL-PPVA@SSM shows multifunctionality in the oil-water separation process. Therefore, it has

the potential value of application in the complex process of wastewater treatment.

As a common living waste produced by households and the catering industry, Kitchen waste oil (KWO) contains a variety of waste animal fats, vegetable oils, salt, and water. According to statistics, the production of kitchen waste has amounted to ~10 million tons annually across China in recent years, which has led to severe environmental pollution. The recycled component has been separated from kitchen waste and can be used directly as fuel, to produce soap, biodiesel, and other industrial products [31–33]. For the recycling of kitchen waste oil, one crucial step in the process of oil-water separation. The CL-PPVA@SSM shows a massive potential to separate KWO/water mixtures. The process and results of complicated kitchen waste separation are indicated in Fig. 14. Due to the remarkable underwater superoleophobicity of the CL-PPVA@SSM, the salty water with a higher density than KWO was quick to permeate the mesh, while KWO was retained on the mesh. Furthermore, oil droplets failed to be observed in the collected water, indicating that the CL-PPVA@SSM was highly effective in the separation of kitchen waste oil from kitchen waste.

4. Conclusions

In conclusion, success was achieved in the fabrication of an underwater superoleophobic and robust superhydrophilic CL-PPVA@SSM using a simple dip-coating method



Fig. 14. Collection process of kitchen waste oil from catering trade by CL-PPVA@SSM.

and crossing reaction. Not only could the CL-PPVA@SSM separate oils from oil-water mixtures with high separation efficiency as high as 99.2%, but it also demonstrates excellent recyclability and high water permeate flux of $467.7 \pm 0.5 \text{ L m}^{-2} \text{ h}^{-1}$ and consequently showed promise for the separation of oil-water mixtures and oil-water emulsions. Additionally, during the oil-water separation process, the CL-PPVA@SSM could also adsorb dyes from the water. The CL-PPVA@SSM exhibited stability under various harsh conditions, and such as abrasion. Importantly, the CL-PPVA@SSM showed a massive potential to separate kitchen waste oil/water mixtures due to the underwater superoleophobic property for the recycling of kitchen waste oil. In brief, the present work indicates encouraging applications to various oil-water separation systems, which is conducive to the environmentally sustainable development and recycling of waste resources.

Acknowledgments

The work was supported by the Scientific Research Foundation of Guilin University of Technology (No. GUTQDJJ2017002) and the Foundation of Key Laboratory of New Processing Technology for Nonferrous Metal & Materials, Guilin University of Technology (19AA).

Author contributions

The manuscript was written through the contributions of all authors. All authors have approved the final version of the manuscript. C. Yang and J. Yang contribute equally to the article.

References

- Z.G. Xu, Y. Zhao, H.X. Wang, X.G. Wang, T. Lin, A superamphiphobic coating with an ammonia-triggered transition to superhydrophilic and superoleophobic for oil-water separation, *Angew. Chem. Int. Ed.*, 54 (2015) 4527–4530.
- Q.L. Ma, H.F. Cheng, Y.F. Yu, Y. Huang, Q.P. Lu, S.K. Han, J.Z. Chen, R. Wang, A.G. Fane, H. Zhang, Preparation of superhydrophilic and underwater superoleophobic nanofiber-based meshes from waste glass for multifunctional oil/water separation, *Small*, 13 (2017) 1700391.
- J.Y. Wu, C.W. Huang, P.S. Tsai, Preparation of poly [3-(methacryloylamino) propyl] trimethylammonium chloride coated mesh for oil-water separation, *Desal. Water Treat.*, 158 (2019) 301–308.
- H. Zhan, T. Zuo, R.J. Tao, C.Y. Chang, Robust tunicate cellulose nanocrystal/palygorskite nanorod membranes for multifunctional oil/water emulsion separation, *ACS Sustainable Chem. Eng.*, 6 (2018) 10833–10840.
- F. Chen, J.L. Song, Z. Liu, J.Y. Liu, H.X. Zheng, S. Huang, J. Sun, W.J. Xu, X. Liu, Atmospheric pressure plasma functionalized polymer mesh: an environmentally friendly and efficient tool for oil/water separation, *ACS Sustainable Chem. Eng.*, 4 (2016) 6828–6837.
- J. Bhadra, N.J. Al-Thani, A. Abdulkareem, The effect of electrospinning parameters on polystyrene nanofiber morphology: oil-water separation, *Desal. Water Treat.*, 111 (2018) 146–154.
- J. Li, X.G. Bai, X.H. Tang, F. Zha, H. Feng, W. Qi, Underwater superoleophobic/underoil superhydrophobic corn cob coated meshes for on-demand oil/water separation, *Sep. Purif. Technol.*, 195 (2018) 232–237.
- H.Q. Li, T. Liang, X.J. Lai, X.J. Su, L. Zhang, X.R. Zeng, Vapor-liquid interfacial reaction to fabricate superhydrophilic and underwater superoleophobic thiolene/silica hybrid decorated fabric for oil/water separation, *Appl. Surf. Sci.*, 427 (2018) 92–101.
- Y.Y. Hou, R.Q. Li, J. Liang, Superhydrophilic nickel-coated meshes with controllable pore size prepared by electrodeposition from deep eutectic solvent for efficient oil/water separation, *Sep. Purif. Technol.*, 192 (2018) 21–29.
- K. Yin, D.K. Chu, X.R. Dong, C. Wang, J.A. Duan, J. He, Femtosecond laser-induced robust periodic nanoripple structured mesh for highly efficient oil-water separation, *Nanoscale*, 9 (2017) 14229–14235.
- T. Yan, X. Chen, T. Zhang, J. Yu, X. Jiang, W. Hu, F. Jiao, A magnetic pH-induced textile fabric with switchable wettability for intelligent oil/water separation, *Chem. Eng. J.*, 347 (2018) 52–63.
- M.J. Liu, S.T. Wang, L. Jiang, Nature-inspired superwettability systems, *Nat. Rev. Mater.*, 2 (2017) 17036.
- C.Y. Cao, M.Z. Ge, J.Y. Huang, S.H. Li, S. Deng, S.N. Zhang, Z. Chen, K.Q. Zhang, S.S. Al-Deyab, Y.K. Lai, Robust fluorine-free superhydrophobic PDMS-ormosil@fabrics for highly effective self-cleaning and efficient oil-water separation, *J. Mater. Chem. A*, 4 (2016) 12179–12187.
- Z. Wang, M. Elimelech, S. Lin, Environmental applications of interfacial materials with special wettability, *Environ. Sci. Technol.*, 50 (2016) 2132–2150.
- J. Li, L. Yan, H. Li, W. Li, F. Zha, Z. Lei, Underwater superoleophobic palygorskite coated meshes for efficient oil/water separation, *J. Mater. Chem. A*, 3 (2015) 14696–14702.
- Z. Xue, S. Wang, L. Lin, L. Chen, M. Liu, L. Feng, L. Jiang, A novel superhydrophilic and underwater superoleophobic hydrogel-coated mesh for oil/water separation, *Adv. Mater.*, 23 (2011) 4270–4273.
- Z.X. Xue, X.W. Xing, S.X. Zhu, W. Zhang, L.Y. Luan, Y.Z. Niu, L.J. Bai, H. Chen, Q. Tao, Underwater superoleophobic porous hydrogel film prepared by soluble salt-template method for oil/water separation in complex environments, *Desal. Water Treat.*, 164 (2019) 151–161.
- Q.D. Zhang, N. Liu, Y. Wei, L. Feng, Facile fabrication of hydrogel coated membrane for controllable and selective oil-in-water emulsion separation, *Soft Matter*, 14 (2018) 2649–2654.
- S.M.A. Soliman, A.M. Ali, M.W. Sabaa, Alginate-based hydrogel for water treatment, *Desal. Water Treat.*, 94 (2017) 129–136.
- Y. An, T. Koyama, K. Hanabusa, H. Shirai, J. Ikeda, H. Yoneno, T. Itoh, Preparation and properties of highly phosphorylated poly(vinyl alcohol) hydrogels chemically cross-linked by glutaraldehyde, *Polymer*, 36 (1995) 2297–2301.
- Y. An, T. Koyama, K. Hanabusa, A. Yamada, H. Shirai, J. Ikeda, H. Yoneno, Preparation of a cation-exchanger based on cross-linked partially phosphorylated poly(vinyl alcohol) and its selectivity for cations, *Kobunshi Ronbunshu*, 52 (1995) 294–298.
- L. Zang, J. Qiu, E. Sakai, C. Yang, In situ preparation of polypyrrole nanorod composite in the presence of phosphorylated polyvinyl alcohol, *Adv. Polym. Tech.*, 34 (2015) 21497.
- H. You, Y. Jin, J. Chen, C. Li, Direct coating of a DKGM hydrogel on glass fabric for multifunctional oil-water separation in harsh environments, *Chem. Eng. J.*, 334 (2018) 2273–2282.
- Z. Du, P. Ding, X. Tai, Z. Pan, H. Yang, Facile preparation of Ag-coated superhydrophobic/superoleophilic mesh for efficient oil/water separation with excellent corrosion resistance, *Langmuir*, 34 (2018) 6922–6929.
- J.Y. Cui, A.T. Xie, S. Zhou, S.W. Liu, Q.Q. Wang, Y.L. Wu, M.J. Meng, J.H. Lang, Z.P. Zhou, Y.S. Yan, Development of composite membranes with irregular rod-like structure via atom transfer radical polymerization for efficient oil-water emulsion separation, *J. Colloid Interface Sci.*, 533 (2019) 278–286.
- X.Y. Chen, D.Y. Chen, N.J. Li, Q.F. Xu, H. Li, J.H. He, J.M. Lu, An I-doped (BiO)₂CO₃ nanosheets-wrapped carbon cloth for highly efficient separation of oil-in-water emulsions, *J. Membr. Sci.*, 567 (2018) 209–215.
- L. Du, X. Quan, X.F. Fan, S. Chen, H.T. Yu, Electro-responsive carbon membranes with reversible superhydrophobicity/

- superhydrophilicity switch for efficient oil/water separation, *Sep. Purif. Technol.*, 210 (2019) 891–899.
- [28] X.J. Yue, T. Zhang, D. Yang, F. Qiu, Z. Li, Superwetting rape pollen layer for emulsion switchable separation with high flux, *Chem. Eng. Sci.*, 203 (2019) 237–246.
- [29] J. Jin, X. Zhao, Y. Du, M. Ding, C. Xiang, N. Yan, C. Jia, Z. Han, L. Sun, Nanostructured three-dimensional percolative channels for separation of oil-in-water emulsions, *iScience*, 6 (2018) 289–298.
- [30] I.I. Enagi, K.A. Al-attab, Z.A. Zainal, Liquid biofuels utilization for gas turbines: a review, *Renewable Sustainable Energy Rev.*, 90 (2018) 43–55.
- [31] A.N. Oumer, M.M. Hasan, A.T. Baheta, R. Mamat, A.A. Abdullah, Bio-based liquid fuels as a source of renewable energy: a review, *Renewable Sustainable Energy Rev.*, 88 (2018) 82–98.
- [32] N. Mansir, S.H. Teo, I. Rabi, Y.H. Taufiq-Yap, Effective biodiesel synthesis from waste cooking oil and biomass residue solid green catalyst, *Chem. Eng. J.*, 347 (2018) 137–144.
- [33] J. Li, Z. Zhao, Y. Shen, H. Feng, Y. Yang, F. Zha, Fabrication of attapulgite coated membranes for effective separation of oil-in-water emulsion in highly acidic, alkaline, and concentrated salty environments, *Adv. Mater. Interfaces*, 4 (2017) 1700364.

Supplementary information

The following are available online, Fig. S1: schematic illustration of the measuring methods of the contact angle, underwater oil contact angle; Fig. S2: the separation efficiency of CL-PPVA@SSM for a series of oil/water emulsion separation; Fig. S3: the separation experiment of hexane-in-water emulsion by the cross-linked PVA@SSM.

S1. Measuring methods of the underwater oil contact angle

The wettability of the surface was measured with water droplets on sample surfaces using a contact angle goniometer (JY-PHb, Chende Jinhe, China) at ambient temperature. For underwater oil contact angles, the samples were placed into a transparent quartzose container that was filled with deionized water. An oil droplet (5 μL) with a higher density than water was directly dropped onto the surface

underwater. For oils with lower density than water, the surfaces were fixed upside down in a quartzose container filled with water, and then the oil droplets were placed beneath the surfaces using an inverted needle. The average contact angle value was obtained by measuring the mesh at three different positions. The sliding angle was characterized by sloped the sample with a 5 μL droplet on it until the droplet started to roll.

S2. Oil/water emulsion separation tests of CL-PPVA@SSM

A series of results of oil/water emulsion separation tests have shown the CL-PPVA@SSM has good separation efficiency as shown in Fig. S2. For comparison, the water-oil separation capability of crosslinked PVA hydrogel coated SS mesh also was investigated under the same conditions. The result was shown in Fig. S3.

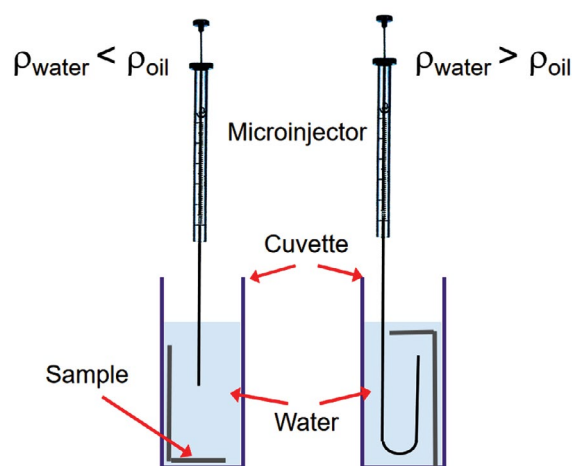


Fig. S1. Schematic illustration of the measuring methods of the contact angle, underwater oil contact angle.

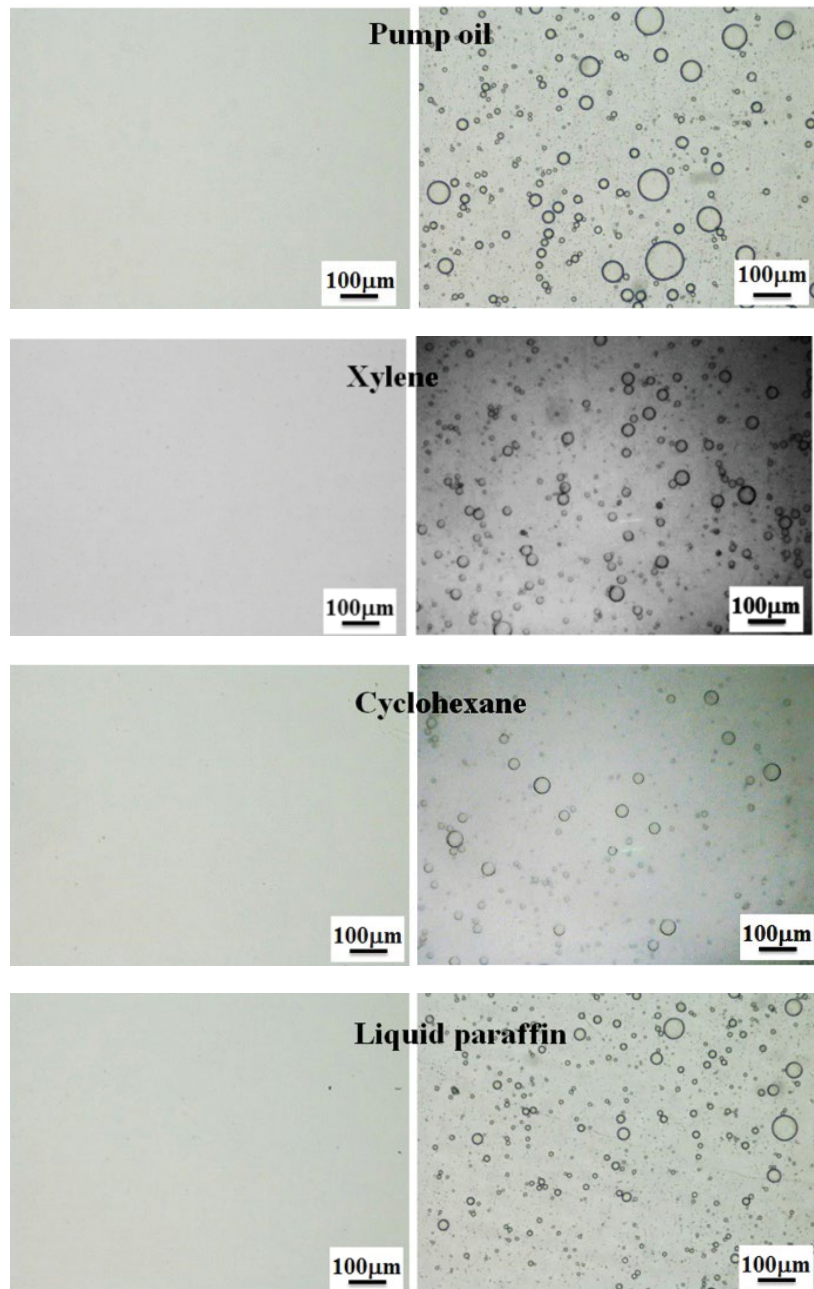


Fig. S2. Separation efficiency of CL-PPVA@SSM for a series of oil/water emulsion separation.

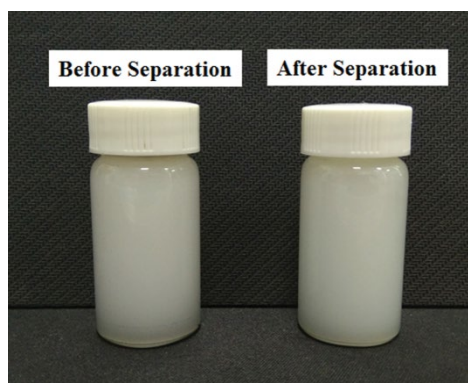


Fig. S3. Separation experiment of hexane-in-water emulsion by the cross-linked PVA @SSM.